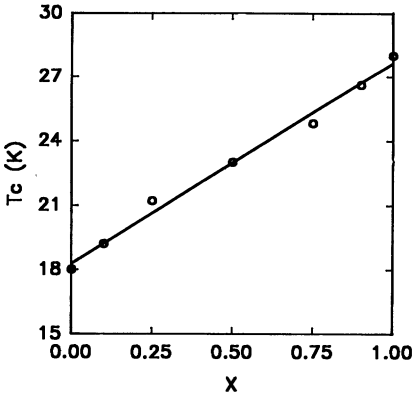

Fig. 4. Plot of T_c versus the Rb:K ratio x in $(Rb_xK_{1-x})_3C_{60}$ materials; the uncertainty in the values of T_c are ±0.2 K.

Because our data now prove that the stoichiometry of the Rb- and K-doped superconducting phases are the same it is important to consider the relationship between these two phases. A classical method to assess experimentally the connectivity between two phases is to study solid solutions, which in the present case correspond to materials with the general formula $(Rb_xK_{1-x})_3C_{60}$. We have prepared these materials using a procedure similar to that employed for the Rb_3C_{60} synthesis. Reaction of $Rb_xK_{1-x}Hg$ alloys with C_{60} in a 3:1 ratio at 200°C produces single-phase superconducting materials in high yields as determined by magnetic susceptibility measurements (Fig. 3). Several important points are evident from these magnetic data. First, analysis of the low temperature shielding values show that the superconducting fractions (x = 0 to 1) are at least 35% for powders; the superconducting fractions of sintered pellets approach 100% (*16*). These data also show no evidence for phase separation (that is, distinct K_3C_{60} and Rb_3C_{60} domains are not formed) within the limits of our sensitivity (0.1 volume percent). Measurements recorded as a function of reaction time further show that rates of Rb and K intercalation must be similar because single-phase materials are obtained for times between 1 and 60 hours. Finally, and perhaps of greatest importance, these data demonstrate that T_c increases systematically with x. As discussed in detail elsewhere (*16*), only Rb and K are incorporated into the C_{60} lattice (for instance, $Rb_xK_{1-x}Tl + C_{60}$ yields similar results), and hence we assign the observed transitions to homogeneous, bulk $(Rb_xK_{1-x})_3C_{60}$ superconducting materials.

We believe that one of the most significant features of our studies is the demonstration of a near linear dependence of T_c with x in these single phase $(Rb_xK_{1-x})_3C_{60}$ materials. These data, which are summarized in Fig. 4, is by no means expected because there has been no clear evidence for mixed alkali-metal intercalation prior to this work. There are several important implications of these new results. First, the continuous evolution of T_c with x in single-phase materials results in the inescapable conclusion that the Rb- and K-doped C_{60} superconducting phases are completely isostructural. Furthermore, these results suggest that there is little preference for Rb versus K occupying the distinct tetrahedral and octahedral sites in the C_{60} lattice (*2, 8*). By way of comparison, it is interesting that the majority of the doping studies of high T_c copper oxide materials have characterized systematic variations in T_c as a function of the hole concentration (*17, 18*). In contrast, our data exhibit a systematic variation in T_c at a constant carrier concentration (assuming that both Rb and K undergo complete charge transfer to C_{60}). We suggest, therefore, that a chemical pressure effect (*19*) provides a viable explanation for these interesting data. Specifically, as x is increased by substituting the larger rubidium ion for K into the solid the lattice expands and the coupling between adjacent C_{60} molecules is reduced; that is, Rb creates a "negative" pressure. This interpretation is supported by recent high-pressure studies of K_3C_{60} which have shown that T_c decreases significantly as the lattice is compressed (*9, 10*). The extreme sensitivity of T_c to pressure, either chemical (this study) or applied externally (*9, 10*), is consistent with a sharply peaked band of electronic states at the Fermi level whose width depends sensitively on the coupling between C_{60} molecules in the lattice.

REFERENCES AND NOTES

1. A. F. Hebard *et al.*, *Nature* **350**, 600 (1991).
2. R. C. Haddon *et al.*, *ibid.*, p. 320.
3. M. J. Rosseinsky *et al.*, *Phys. Rev. Lett.* **66**, 2830 (1991).
4. K. Holczer *et al.*, *Science* **252**, 1154 (1991).
5. P. J. Benning *et al.*, *ibid.*, p. 1417.
6. S. P. Kelty *et al.*, *J. Phys. Chem.*, in press.
7. O. Zhou *et al.*, *Nature* **351**, 462 (1991).
8. P. W. Stephens *et al.*, *ibid.*, p. 632.
9. J. E. Schirber *et al.*, *Physica C*, in press.
10. G. Sparn *et al.*, *Science* **252**, 1829 (1991).
11. K. Holczer *et al.*, *Phys. Rev. Lett.* **67**, 271 (1991).
12. S. P. Kelty, C. C. Chen, C. M. Lieber, *Nature* **352**, 223 (1991).
13. W. Krätschmer *et al.*, *ibid.* **347**, 254 (1990).
14. R. E. Haufler *et al.*, *J. Phys. Chem.* **94**, 8634 (1990).
15. F. Diederich *et al.*, *Science* **252**, 548 (1991).
16. S. P. Kelty, C. C. Chen, C. M. Lieber, in preparation. Tl metal has been detected by x-ray diffraction following reaction of MTl with C_{60}, and thus shows that it is not substituted into the C_{60} lattice under these conditions. Additionally, diffraction studies show that K_3C_{60} and Rb_3C_{60} have similar fcc (face-centered-cubic) lattices.
17. R. J. Cava, *Science* **247**, 656 (1990).
18. M.-H. Whangbo and C. C. Torardi, *Acc. Chem. Res.* **24**, 127 (1991).
19. J. M. Williams *et al.*, *Prog. Inorg. Chem.* **35**, 51 (1987).

18 July 1991; accepted 31 July 1991

Interpretation of Snow-Climate Feedback as Produced by 17 General Circulation Models

R. D. CESS, G. L. POTTER, M.-H. ZHANG, J.-P. BLANCHET, S. CHALITA, R. COLMAN, D. A. DAZLICH, A. D. DEL GENIO, V. DYMNIKOV, V. GALIN, D. JERRETT, E. KEUP, A. A. LACIS, H. LE TREUT, X.-Z. LIANG, J.-F. MAHFOUF, B. J. MCAVANEY, V. P. MELESHKO, J. F. B. MITCHELL, J.-J. MORCRETTE, P. M. NORRIS, D. A. RANDALL, L. RIKUS, E. ROECKNER, J.-F. ROYER, U. SCHLESE, D. A. SHEININ, J. M. SLINGO, A. P. SOKOLOV, K. E. TAYLOR, W. M. WASHINGTON, R. T. WETHERALD, I. YAGAI

Snow feedback is expected to amplify global warming caused by increasing concentrations of atmospheric greenhouse gases. The conventional explanation is that a warmer Earth will have less snow cover, resulting in a darker planet that absorbs more solar radiation. An intercomparison of 17 general circulation models, for which perturbations of sea surface temperature were used as a surrogate climate change, suggests that this explanation is overly simplistic. The results instead indicate that additional amplification or moderation may be caused both by cloud interactions and longwave radiation. One measure of this net effect of snow feedback was found to differ markedly among the 17 climate models, ranging from weak negative feedback in some models to strong positive feedback in others.

THE MOST COMPREHENSIVE WAY TO infer future climate change, caused by increasing greenhouse gases, is by means of three-dimensional general circulation models (GCMs). The climate responses of existing GCMs, however, to increasing atmospheric CO_2 differ considerably (*1*), as is consistent with a GCM intercomparison study that addressed two interactive climate feedback mechanisms: water vapor feedback and cloud feedback (*2, 3*). The former is a positive feedback because climate warming produces an increase in atmospheric water vapor, itself a greenhouse gas, that amplifies

Table 1. Summary of the GCMs used in the intercomparison (7). NCAR CCM, National Center for Atmospheric Research Community Climate Model.

Model	Investigators
Bureau of Meteorology Research Centre, Melbourne (BMRC)	McAvaney, Rikus, and Colman
Canadian Climate Centre (CCC)	Blanchet
Colorado State University (CSU)	Randall and Dazlich
Department of Numerical Mathematics of the USSR Academy of Sciences (DNM)	Dymnikov and Galin
Direction de la Météorologie Nationale, Toulouse (DMN)	Mahfouf and Royer
European Centre for Medium-Range Weather Forecasts (ECMWF)	Potter, Slingo, and Morcrette
European Centre for Medium-Range Weather Forecasts; Max Planck Institute for Meteorology, Hamburg (ECHAM)	Roeckner, Schlese, and Keup
Geophysical Fluid Dynamics Laboratory (GFDL)	Wetherald
Institute for Atmospheric Physics, Beijing; State University of New York (IAP/SUNY)	Liang
Laboratoire de Météorologie Dynamique, Paris (LMD)	Le Treut and Chalita
Main Geophysical Observatory, Leningrad (MGO)	Meleshko, Sokolov, and Sheinin
Meteorological Research Institute, Japan (MRI)	Yagai
NASA Goddard Institute for Space Studies (GISS)	Del Genio and Lacis
NCAR CCM, Version 0 (CCM0)	Washington
NCAR CCM; Lawrence Livermore National Laboratory (CCM/LLNL)	Taylor and Norris
Oregon State University; IAP (OSU/IAP)	Zhang and Cess
United Kingdom Meteorological Office (UKMO)	Mitchell and Jerrett

the warming. The GCM intercomparison study (*2, 3*) showed that the models were in remarkable agreement with respect to this positive feedback, but inclusion of cloud feedback caused a roughly threefold variation among the models in one measure of climate sensitivity. There was no consistency even with respect to the sign of cloud feedback. In this study we have examined a third climate feedback mechanism: snow feedback. This is conventionally regarded as a positive feedback, because climate warming reduces snow cover over land areas, resulting in a less reflective planet that in turn absorbs more solar (shortwave) radiation. Although this description is physically obvious, it does not explicitly include the possibility of both cloud interactions and longwave feedback as induced by a decrease in snow cover.

As before (*2, 3*), we concentrated on the global climate sensitivity parameter λ, which relates the change in global-mean surface temperature ΔT to the direct radiative forcing G that induces the change in climate, so that

$$\Delta T = \lambda G \quad (1)$$

with

$$G = \Delta F - \Delta Q \quad (2)$$

where F and Q, respectively, denote the global-mean emitted longwave (LW) and net downward shortwave (SW) fluxes at the top of the atmosphere (TOA). Thus ΔF and ΔQ represent the climate-change TOA responses to G. Furthermore,

$$\lambda = \frac{1}{\Delta F/\Delta T - \Delta Q/\Delta T} \quad (3)$$

An increase in λ thus represents an increased climate change due to a given climate forcing G as induced, for example, by an increase in atmospheric CO_2 concentration (*1*).

As before (*2, 3*), for the sole purpose of intercomparing climate sensitivity, we adopted ± 2 K perturbations in sea surface temperature (SST) in conjunction with perpetual month simulations as a surrogate climate change. This procedure is in effect an inverse climate-change simulation. Rather than introduce a direct forcing G into the models and then let the climate respond to this forcing, we instead prescribed the climate change (ΔSST = 4 K) and let the models in turn produce their respective forcings in accordance with Eq. 2. We isolated cloud effects as before (*2, 3*) by separately averaging a model's clear-sky TOA fluxes, so that in addition to evaluating climate sensitivity for the globe as a whole we also were able to consider an equivalent "clear-sky" Earth.

The clear-sky TOA fluxes, however, were evaluated differently in this case. Previously they were calculated from the subset of grid points (or fractional grid areas) in which there was no cloud. In this case there can be a spurious surface albedo feedback caused by climate-induced changes in the geographical location of these clear-sky regions (*3*). To avoid confusing this with snow feedback, we alternatively adopted the method II procedure (*4*) by which clear-sky TOA fluxes are computed at each grid point from a second radiation calculation with no clouds present in the atmospheric column (but with the remaining quantities unchanged). This procedure in addition avoids potential sampling errors associated with diurnal cloud variability (*5*).

The earlier perpetual July simulation was chosen to suppress snow feedback (*2, 3*); to study its effect we chose a perpetual April simulation, as suggested by sensitivity studies with a single model (OSU/IAP in Table 1). Although there is more Northern Hemisphere snow cover in January than in April, there is less solar radiation over regions where the snow line retreats. Moreover, this model actually produced a greater warming-induced reduction in snow cover for April than for January. Sea ice was again held fixed so as to focus on snow feedback.

We should emphasize that snow feedback for a perpetual April is not an analog for actual climate change; a perpetual month does not replicate the annual cycle. Nor are uniform SST perturbations representative of climate change, because they do not account for changes in pole-to-equator temperature gradients. Our point is that, if the models were consistent in their depiction of snow

R. D. Cess and M.-H. Zhang, Institute for Terrestrial and Planetary Atmospheres, State University of New York, Stony Brook, NY 11794.
G. L. Potter and K. E. Taylor, Lawrence Livermore National Laboratory, Livermore, CA 94550.
J. P. Blanchet, Canadian Climate Centre, Downsview, Ontario, Canada M3H 574.
S. Chalita and H. Le Treut, Laboratoire de Météorologie Dynamique, 24 Rue Lhomond, 75231 Paris Cédex 05, France.
R. Colman, B. J. McAvaney, L. Rikus, Bureau of Meteorology Research Centre, GPO Box 1289K, Melbourne, 3001 Victoria, Australia.
D. A. Dazlich and D. A. Randall, Colorado State University, Fort Collins, CO 80523.
A. D. Del Genio and A. A. Lacis, National Aeronautics and Space Administration (NASA) Goddard Institute for Space Studies, 2880 Broadway, New York, NY 10025.
V. Dymnikov and V. Galin, Department of Numerical Mathematics, USSR Academy of Sciences, 29 Ryleeva Street, Moscow 119034, USSR.
D. Jerrett and J. F. B. Mitchell, The Hadley Centre for Climate Prediction and Research, Meteorological Office, Bracknell, Berkshire RG12 2SZ, England.
E. Keup, E. Roeckner, U. Schlese, Max Planck Institute for Meteorology, Bundestrasse 55, D2000, Hamburg 13, Federal Republic of Germany.
X.-Z. Liang, State University of New York, Albany, NY 12205.
J.-F. Mahfouf and J.-F. Royer, Direction de la Météorologie Nationale, Centre National de Recherches Metallurgiques (CNRM), 42 Avenue Coriolis, 31057 Toulouse Cédex, France.
V. P. Meleshko, D. A. Sheinin, A. S. Sokolov, Voeikov Main Geophysical Observatory, 7 Karbisheva, Leningrad 194018, USSR.
J.-J. Morcrette, European Centre for Medium-Range Weather Forecasts, Reading, Berkshire RG2 9AX, England.
P. M. Norris, Scripps Institution of Oceanography, University of California, San Diego, La Jolla, CA 92093.
J. M. Slingo, University of Reading, Reading, Berkshire RG6 2AU, England.
W. M. Washington, National Center for Atmospheric Research, Boulder, CO 80307.
R. T. Wetherald, Princeton University, National Oceanic and Atmospheric Administration–Geophysical Fluid Dynamics Laboratory, Post Office Box 308, Princeton, NJ 08540.
I. Yagai, Meteorological Research Institute, 1-1, Nagamine, Tsukuba, Ibaraki-ken 305, Japan.

feedback for, say, CO_2-induced warming, they should also exhibit consistency for the perpetual April simulations. Our goal was to use the perpetual April simulation solely as a vehicle for intercomparing and interpreting one measure of snow feedback as produced by a number of GCMs, fully realizing that this snow-feedback surrogate is not representative of CO_2-induced warming.

To isolate snow feedback, two sets of April climate-change simulations were performed, one for which the snow line was allowed to retreat for the $\Delta SST = -2$ K to +2 K climate change and the other for which the snow cover was held fixed at that for the $\Delta SST = -2$ K simulation. The difference in λ between these two cases is thus a measure of snow feedback. Specifically, if we let the subscript s denote the fixed snow case, then a positive departure of λ/λ_s from unity is a measure of positive snow feedback.

The 17 GCMs used in this intercomparison (designated by acronyms in Table 1) are nearly the same as those used earlier (*6*), although several models have been subsequently modified (7). All the models are similar in the way they form snow. If the temperature of the lowest atmospheric level is below freezing, then precipitation falls as snow, although the BMRC, DMN, DNM, ECMWF, and ECHAM models contain slight variants to this procedure. The snow depth is computed as a balance of snowfall, melting, and sublimation. The similarities, however, end there, because the snow albedos are treated quite differently among the models. For CCM/LLNL (*8*) only half of a snow-covered grid area is assigned the albedo of snow; the other half retains the bare-ground albedo. In the various models the snow albedo can be a function of one or more of the following quantities: snow depth, age, and temperature. In addition, the snow albedo is, in some models, substantially reduced for forested regions. Because of these differences in snow albedo formulations, the areal extent of snow and its warming-induced change do not, by themselves, relate to intermodel differences in snow feedback.

Table 2. Summary of climate sensitivity parameters λ_c and λ for the perpetual April simulations; these have the units of K m^2 W^{-1}. The numbers on the left refer to the model numbers in Figs. 1 through 3. These are ordered in terms of increasing values of the snow feedback parameter λ/λ_s. In addition to global (that is, entire Earth) results for both fixed and variable snow, comparable clear-sky sensitivity parameters, denoted by λ_c, are also given.

Model	Fixed snow		Variable snow	
	λ_c	λ	λ_c	λ
1. CSU	0.46	0.39	0.47	0.36
2. GFDL	0.56	0.60	0.57	0.56
3. ECMWF	0.48	0.42	0.56	0.40
4. CCM/LLNL	0.48	0.88	0.54	0.86
5. DNM	0.44	0.47	0.49	0.46
6. GISS	0.54	0.90	0.60	0.94
7. CCC	0.45	0.41	0.51	0.44
8. IAP/SUNY	0.54	0.59	0.59	0.65
9. ECHAM	0.46	0.54	0.53	0.60
10. DMN	0.43	0.57	0.47	0.65
11. MRI	0.57	0.84	0.68	0.95
12. LMD	0.61	1.09	0.63	1.28
13. MGO	0.46	0.56	0.66	0.69
14. BMRC	0.45	0.37	0.59	0.46
15. UKMO	0.55	0.57	1.09	0.82
16. OSU/IAP	0.35	0.83	0.41	1.35
17. CCM0	0.56	1.49	0.89	2.83
Mean	0.49	0.68	0.60	0.84
SD	0.07	0.30	0.17	0.59

An intercomparison of climate sensitivity parameters showed significant variability among the models (Table 2). The departure of λ/λ_c from unity is a measure of cloud feedback, and $\lambda/\lambda_c > 1$ indicates a positive feedback (*2, 3*). The fixed-snow λ_c results, for which there is neither cloud nor snow feedback, are in good agreement and produce a standard deviation (SD) of only 0.07 K m^2 W^{-1}; it is increased to 0.30 K m^2 W^{-1} when cloud feedback is included. This is consistent with the earlier July simulations (*2, 3*), again indicating that cloud feedback is a major contributor to intermodel differences. By itself snow feedback produces more modest differences (SD = 0.17 K m^2 W^{-1}) than does cloud feedback. But it roughly doubled the SD for both the clear and the global cases, and this effect demonstrates the interactive nature of these feedbacks.

The snow feedback parameter λ/λ_s varied considerably among the models (Fig. 1A, filled circles), and curiously five models exhibited a weak negative feedback. Such an effect is attributed to cloud interactions, because the clear-sky λ/λ_s is greater than unity for all models (Fig. 1A, open circles), although intermodel differences are still substantial. In general, clouds are thought to reduce positive snow feedback by shielding the TOA albedo change. This mechanism, however, cannot account for the results of models 1 through 5, nor can it account for the cloud-induced amplification of positive snow feedback for models 10, 12, 16, and 17.

In order to understand the reasons for the above behavior, let us express the snow feedback parameter λ/λ_s, through use of Eq. 3, as

$$\lambda/\lambda_s = (\Delta T/\Delta T_s)(1 + \mathrm{SRR}/G) \quad (4)$$

where ΔT_s is the change in global-mean surface temperature for the fixed snow simulation. The quantity SRR (snow-radiative response) represents the effect of snow retreat on the TOA radiation balance, so that

$$\mathrm{SRR} = (\Delta Q - \Delta Q_s) - (\Delta F - \Delta F_s) \quad (5)$$

The SRR incorporates both the SW and LW contributions to the snow-induced TOA radiative perturbation. Because the term (1 + SRR/G) in Eq. 4 acts as a snow-feedback multiplier to the direct forcing G, then SRR/G is a specific measure of snow feedback. Intermodel differences in SRR/G (Fig. 1B) cause most of the differences in λ/λ_s (Fig. 1A).

The direct radiative perturbation caused by the snow retreat is the SW component of SRR. There are substantial intermodel differences in this quantity for clear-sky conditions (Fig. 2A), and the clear versus global comparisons demonstrate that cloud interactions are also significant. In addition to cloud shielding, which can only moderate the magnitude of the SW component of SRR, there also can be a redistribution of cloud cover (*9*). If, for example, as the snow retreats there is a simultaneous increase in cloud cover over bare land, then this would act counter to the TOA albedo reduction directly caused by snow retreat. It is this effect, possibly combined with changes of cloud optical properties, that evidently has produced the clear versus global sign reversal for models 1 and 3 (Fig. 2A) and consequently negative snow feedback (Fig. 1A). The lack of any net cloud interaction for model 14 implies that amplification by cloud redistribution exactly compensates for shielding, whereas there is a slight overcompensation for models 9, 10, and 16.

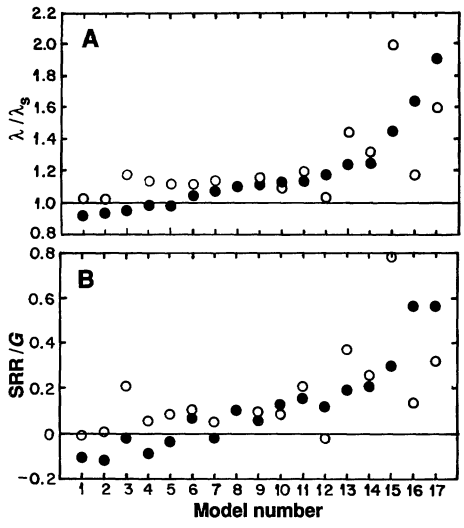

Fig. 1. (**A**) The snow feedback parameter λ/λ_s for the 17 GCMs and for both global (●) (entire Earth) and clear (○) designations. For model 8 the global and clear values are the same. (**B**) Values of SRR/G for the 17 GCMs and for both global and clear designations.

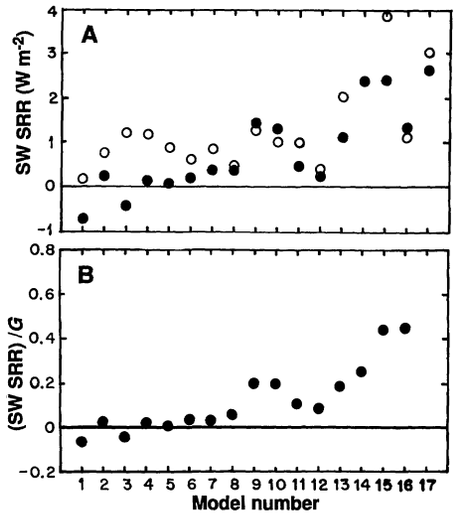

Fig. 2. (**A**) The shortwave component of snow-radiative response (SW SRR) for the 17 GCMs and for both global (●) (entire Earth) and clear (○) designations. For model 14 the global and clear values are the same. (**B**) Values of (SW SRR)/G for the 17 GCMs. For model 17 (not shown) the value is 1.57.

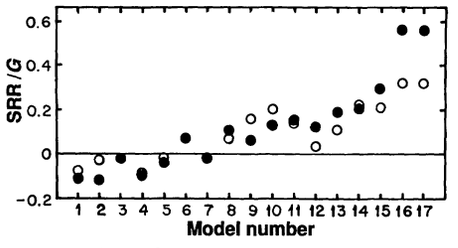

Fig. 3. Values of SRR/G for the 17 GCMs with (●) and without (○) longwave snow feedback. For models 3, 6, and 7 LW snow feedback has no effect.

Clouds produce yet a further impact on snow feedback because feedback mechanisms are interactive. Models 10 and 16 yield comparable SW SRR, both clear and global (Fig. 2A), as is consistent with the similar clear-sky snow feedback of the two models (Fig. 1A). Model 16, however, yields much stronger global snow feedback because its cloud feedback is greater and thus its fixed-snow sensitivity is larger (Table 2). As a result, the global SW SRR of model 16, although comparable to that of model 10, has a greater climate impact that results in enhanced snow feedback. The quantity SRR/G (Eq. 4) includes this effect, because normalizing SRR by G accounts for differences in model sensitivity (*10*). Indeed, intermodel differences in (SW SRR)/G (Fig. 2B) account for much of the differences in global λ/λ_s (Fig. 1A). But there are also significant differences in the direct radiative perturbation as represented by SW SRR (Fig. 2A), so that even if all the models had the same cloud feedback they still would produce substantially different snow feedback.

Further intermodel differences are caused by the LW component of SRR

$$\text{LW SRR} = \Delta F_s - \Delta F = \text{SRR} - \text{SW SRR} \quad (6)$$

as is evident by comparison of the results in Figs. 1B and 2B. Note that (SW SRR)/G is weakly positive for models 2, 4, and 5 (Fig. 2B), whereas inclusion of the LW component of SRR reverses the sign (Fig. 1B, filled circles). Thus it is the LW component of SRR that causes negative snow feedback in these three models (Fig. 1A). But simply intercomparing LW SRR provides little physical insight, because there are two distinctly different processes involved. To demonstrate this, Eq. 6 may be rephrased as

$$\text{LW SRR} = (\Delta F/\Delta T)_s(\Delta T_s - \Delta T) + [(\Delta F/\Delta T)_s - (\Delta F/\Delta T)]\Delta T \quad (7)$$

If $\Delta F/\Delta T = (\Delta F/\Delta T)_s$, then snow retreat does not alter the LW feedback and LW SRR is represented by the first term in Eq. 7, which is the direct contribution caused by the snow-induced change in land temperature. It is the second term in Eq. 7 that is of interest, because, if the two LW response derivatives differ, then snow retreat introduces an LW snow feedback as represented by this term.

To demonstrate this effect, we obtained values represented by the open circles (Fig. 3) by computing LW SRR, using only the first term in Eq. 7; thus contributions from LW snow feedback were eliminated. Several models exhibit significant LW snow feedback (Fig. 3). The modest positive snow feedback of model 12 was due mostly to LW feedback, whereas it was a strong contributor to the positive snow feedbacks of models 16 and 17. The positive LW feedback in model 16 occurred because snow retreat caused a steeper lapse rate so that the colder atmosphere emitted less LW radiation. A similar diagnosis has not been performed for the other models.

The analysis shows that snow feedback involves two separate climate responses: the direct effect as manifested by the clear SW SRR and indirect effects caused by cloud interactions and LW feedback. The models are markedly different with respect to the direct effect (Fig. 2A, open circles), and changing this effect within a model will alter the indirect effects. To demonstrate this we have replaced the snow albedo formulation in model 16 by that of model 1, and as with model 1 we found that the revised model 16 produced a near-negligible direct effect. This albedo transfer, however, substantially increased the indirect effects, with the result that net (direct plus indirect) snow feedback was actually increased. It must be further emphasized that the direct effect can depend on aspects of a model other than the snow albedo formulation, because snow depth is computed as a balance of snowfall, melting, and sublimation. For example, although models 8 and 16 contain the same snow albedo formulation, their direct effects differ considerably (Fig. 2A).

This study thus demonstrates that snow feedback is associated with a multitude of complexities, and that it cannot simplistically be ascribed solely to an albedo change induced by snow retreat. Clouds are a significant cause of interactive effects, such as cloud redistribution that in some models produces a sign reversal of this feedback, which in other models occurs as a consequence of cloud-induced LW interactions. Also in some models there is a significant LW feedback associated with snow retreat. By using a diversity of climate models we have been able to understand better the potential interactive processes associated with snow feedback, a necessary first step in identifying ways of improving the models.

REFERENCES AND NOTES

1. *Climate Change, The IPCC* [*Intergovernmental Panel on Climate Change*] *Scientific Assessment*, J. T. Houghton, G. J. Jenkins, J. J. Ephraums, Eds. (Cambridge Univ. Press, Cambridge, 1990), chap. 3, pp. 69–92.
2. R. D. Cess *et al.*, *Science* **245**, 513 (1989).
3. R. D. Cess *et al.*, *J. Geophys. Res.* **95**, 16601 (1990).
4. R. D. Cess and G. L. Potter, *Tellus Ser. A* **39**, 460 (1987).
5. D. A. Randall *et al.*, *J. Atmos. Sci.* **46**, 1922 (1989); G. L. Potter *et al.*, in preparation.
6. Of the 19 GCMs used in (*3*), two were different versions of the GFDL model and only one of these, GFDL I in (*3*), was used in the present study. The two models from (*3*) that are missing are the OSU/LLNL GCM, which is no longer maintained, and CCM1 which is being replaced by a newer version. One model (IAP/SUNY) has been added to the present investigation. This is a nine-level finite-difference model having a horizontal resolution of 4° latitude by 5° longitude.
7. With the exception of IAP/SUNY, brief descriptions of the GCMs are given in (*3*). Several of the models (BMRC, CCC, CSU, DNM, ECMWF, ECHAM, MGO, and LMD) contain subsequent modifications, descriptions of which are available from the respective investigators.
8. The CCM/LLNL is derived from the National Center for Atmospheric Research (NCAR) CCM Version 1 that originally contained an error in the latent heat of fusion. This was corrected in recent versions of the CCM as well as the CCM/LLNL. Results shown for CCM/LLNL represent a 50-day average following a 40-day spin-up period. Recently the simulation has been extended, and longer term fluctuations have been found that may modify these results.
9. W. J. Ingram *et al.*, *J. Geophys. Res.* **94**, 8609 (1989).
10. In the present context by which comparable climate change is prescribed (ΔSST = 4 K) for all the models, then increased climate sensitivity results in a smaller G that by itself increases SRR/G.

11. Valuable suggestions were provided by G. J. Boer and W. L. Gates. This study was performed under

the auspices of the Atmospheric and Climate Research Division, U.S. Department of Energy, under grant DE-FG02-85ER60314 to State University of New York, Stony Brook, contract W-7405-ENG-48 to Lawrence Livermore National Laboratory, contract DE-FG02-89ER-69027 to Colorado State University, interagency agreement DE-AI05-90ER61068 to Goddard Institute for Space Studies, and contract DE-AI01-80EV10220 to the National Center for Atmospheric Research, which is sponsored by the National Science Foundation. Further support was provided by NASA's Climate Program under grant NAG 5-1058 to Colorado State University, by the Bundesminister für Forschung und Technologie, Federal Republic of Germany, through grant KFT 05/6 to the University of Hamburg, by the French Climate Program (PNEDC) and the Commission of European Communities through contract EV4C-0066-F to DMN/CNRM, and by a grant through the University of California Institutional Collaborative Research Program to Scripps Institution of Oceanography. Computing resources were also provided to Colorado State University by the Numerical Aerodynamic Simulation Program at NASA Ames Research Center.

12 April 1991; accepted 14 June 1991

Declining Amphibian Populations: The Problem of Separating Human Impacts from Natural Fluctuations

JOSEPH H. K. PECHMANN,* DAVID E. SCOTT, RAYMOND D. SEMLITSCH, JANALEE P. CALDWELL, LAURIE J. VITT, J. WHITFIELD GIBBONS

Reports of declining amphibian populations in many parts of the world are numerous, but supporting long-term census data are generally unavailable. Census data from 1979 to 1990 for three salamander species and one frog species at a breeding pond in South Carolina showed fluctuations of substantial magnitude in both the size of breeding populations and in recruitment of juveniles. Breeding population sizes exhibited no overall trend in three species and increased in the fourth. Recent droughts account satisfactorily for an increase in recruitment failures. These data illustrate that to distinguish between natural population fluctuations and declines with anthropogenic causes may require long-term studies.

EVALUATION OF THE REPORTED DECLINES of amphibian populations, some possibly to extinction (*1*), has been hampered by the dearth of long-term census data on amphibians. Conclusions of National Research Council workshop participants about the status of amphibian populations (*1*) were based primarily on anecdotal observations. These observations have convinced many that there is a general decline worldwide, although not all species and regions appear to be affected (*1, 2*). In many individual cases, however, it may be difficult to distinguish declines resulting from human activities from natural population fluctuations without long-term data on the natural variation in both real and apparent (catchable) population sizes (*2*).

We have monitored amphibian populations at one ephemeral pond, Rainbow Bay, continuously for the past 12 years, the period during which most of the reported declines have occurred (*1*). Although data from one site cannot be extrapolated to other sites, Rainbow Bay nonetheless provides an important test site for the amphibian decline question because of the extensive data available.

Rainbow Bay is a Carolina bay (*3, 4*) located on the U.S. Department of Energy's 780-km^2 Savannah River Site (*4*) in the upper coastal plain sandhills region in South Carolina. The pond is approximately 1 ha with a maximum water depth of 1.04 m and usually fills during the winter and dries each spring or summer (*5*). Rainbow Bay and the adjacent terrestrial habitats were protected from most human impacts during our 12-year study, but were altered in the past (*6*). Anthropogenic factors have been implicated in many of the reported declines and extinctions of amphibian populations, yet others have occurred in protected, seemingly pristine areas (*1*). Thus, Rainbow Bay's current protected status does not make it an exception with respect to its potential for amphibian declines.

Amphibians migrating to and from the pond have been censused since 21 September 1978 with the use of a terrestrial drift fence with pitfall traps that completely surrounds the pond (*7*). Traps are checked daily, and data to 31 August 1990 are reported here. Upon capture, all amphibians were identified, marked by clipping toes, and released on the opposite side of the fence from where captured.

Five species of salamanders and 11 species of frogs and toads are known to have bred at Rainbow Bay (*5*). We report data on *Ambystoma opacum* (marbled salamander), *A. talpoideum* (mole salamander), *A. tigrinum tigrinum* (eastern tiger salamander), and *Pseudacris ornata* (ornate chorus frog). These species were chosen because demographic interpretation of the drift-fence data is most straightforward for them (*8*). The four are primarily terrestrial and fossorial except for the aquatic larval stage (*9*). Reproductive *A. opacum* migrate to breeding ponds from September to November, whereas breeding migrations of the other three species occur primarily from November to March. Adults spend a few days to weeks at the pond before returning to terrestrial habitats (*10*). Juveniles metamorphose and emigrate from the pond during the following spring and summer. Age at first reproduction varies considerably, but some individuals of all four species reproduce at 1 year of age (*11, 12, 13*).

These species usually return to their natal pond to breed, that is, they are philopatric (*13, 14*). Four smaller breeding sites occur within 1 km of Rainbow Bay, and low rates of dispersal connect populations of these species to form metapopulations (*15*). Immigration and emigration are usually minor components of the population dynamics of these philopatric species, but may be important in long-term persistence (*15*).

Because individuals of the four species cannot trespass the drift fence, this technique provides a nearly complete census of breeding adults and juvenile recruits. Terrestrial immatures and adults that skip breeding are not censused, however. Breeding populations had approximately 1 to 1 or male-biased sex ratios each year; therefore only data for females are presented. We tested for evidence of a decline in numbers of breeding females or of metamorphosing juveniles.

Female breeding population sizes fluctuated over three orders of magnitude among years, and juvenile recruitment over five (Fig. 1). Each species was common in some years but uncommon or absent in others. Year-to-year variation and short-term trends make it difficult to discern long-term trends. Breeding populations declined during some time periods, but increased during others (Fig. 1). Fluctuations in breeding population sizes were not significantly correlated among species (*16*).

Breeding population sizes vary more than adult population sizes. Adults migrate to ponds only during warm night rains within their breeding season and may skip breeding in years of low rainfall (*13, 17*). For example, breeding populations of *A. talpoideum*, *A. tigrinum*, and *P. ornata* were reduced in

J. H. K. Pechmann, Savannah River Ecology Laboratory, University of Georgia, P.O. Drawer E, Aiken, SC 29802, and Department of Zoology, Duke University, Durham, NC 27706.
D. E. Scott and J. W. Gibbons, Savannah River Ecology Laboratory, University of Georgia, P.O. Drawer E, Aiken, SC 29802.
R. D. Semlitsch, Zoologisches Institut der Universität Zürich, Winterthurerstrasse 190, CH-8057, Zürich, Switzerland.
L. J. Vitt and J. P. Caldwell, Oklahoma Museum of Natural History and Department of Zoology, University of Oklahoma, Norman, OK 73019.

*To whom all correspondence should be addressed.